

# Microstructural analysis of hard amorphous carbon films deposited with high-energy ion beams

R.S. Brusa<sup>a</sup>, A. Somoza<sup>b,\*</sup>, H. Huck<sup>c</sup>, N. Tiengo<sup>a</sup>, G.P. Karwasz<sup>a</sup>, A. Zecca<sup>a</sup>,  
M. Reinoso<sup>c</sup>, E.B. Halac<sup>c</sup>

<sup>a</sup> *Istituto Nazionale per la Fisica della Materia, Dipartimento di Fisica, Università di Trento, 38050 Povo, Trento, TN, Italy*

<sup>b</sup> *IFIMAT, Universidad Nacional del Centro de la Provincia de Buenos Aires and Comisión de Investigaciones Científicas de la Provincia de Buenos Aires, Pinto 399, 7000 Tandil, Argentina*

<sup>c</sup> *Departamento de Física, Comisión Nacional de Energía Atómica, Av. Del Libertador 8250, 1429 Buenos Aires, Argentina*

Received 9 January 1999; accepted 28 April 1999

## Abstract

Hard amorphous carbon films produced using high-energy (ca. 30 keV) ion beam deposition of  $\text{CH}_3^+$  and  $\text{CH}_4^+$  on silicon wafers, have been investigated by Positron Annihilation Spectroscopy (PAS), the results are correlated with Raman Spectroscopy and Electrical Resistivity measurements. The microstructural modifications of the films as a function of the annealing temperature in the 300–600°C range have been studied. The evolution of the fractions of  $\text{sp}^2$  and  $\text{sp}^3$  bonds is described and related to the changes of the open volume defect distribution and the graphitization process. © 1999 Elsevier Science B.V. All rights reserved.

PACS: 61.40.+b; 68.55.Jk; 78.70.Bj; 78.30.-j

Keywords: Hard amorphous carbon films; Defects; Graphitization; Positron annihilation; Raman spectroscopy; Electrical resistivity

## 1. Introduction

Hard amorphous carbon (a-C) films are interesting materials from the point of view of their physical and chemical properties, which are close to those of a diamond. These films can be obtained in a variety of ways and their properties depend on the deposition method; many experimental techniques have been applied in order to characterize the different films so obtained.

The nature of the bonding in this material is of particular interest to understand the macroscopic properties. Electron energy loss spectroscopy (EELS), Auger electron spectroscopy (AES) and X-ray photoelectron spectroscopy (XPS) give information about the nature of the local bonding of the carbon films, i.e., the distribution of atoms among  $\text{sp}^3$  and  $\text{sp}^2$  configurations [1]. Electron, X-ray and neutron diffraction methods are used to evaluate structural information of amorphous carbon (atomic distances and bond angles). The composition of these films can be monitored using Rutherford backscattering spectroscopy (RBS) and the presence of hydro-

\* Corresponding author. Fax: +54-2293-444190; E-mail: asomoza@exa.unicen.edu.ar

gen by elastic recoil spectroscopy (ERDA) [2]. Raman spectroscopy is probably the most common technique to evaluate the amorphous character of these films [3].

In recent papers [4,5] we have characterized the structure and thermal behavior of a-C films obtained using high energy ion beam deposition methods by means of EELS, AES, XPS, ERDA and Raman spectroscopy. The microscopic structure consists of an amorphous intricate network of  $sp^2$  and  $sp^3$  C–C bonds. It is of particular interest to understand the evolution of this structure with the temperature. Raman spectra showed that graphitization starts at about 450°C [6]. In this work we follow the structural change upon annealing heat treatments by means of positron annihilation spectroscopy (PAS), Raman spectroscopy and electrical resistivity measurements.

PAS was demonstrated to be one of the most powerful techniques in depth profiling of open volume defects (from vacancies to voids) in semiconductors [7]. Positrons, injected in a solid at kilo-electron-volts energies, slow down reaching thermal energies in few picoseconds; after thermalization they diffuse and are efficiently trapped by open volume defects, if present. Finally, they annihilate. The annihilation gamma rays carry information about the momentum of the positron-electron annihilating pair.

Only recently, this technique has been applied in the study of amorphous thin films. In particular, the distribution of point defects induced by nitrogen implantation in a-C:H films [8], the distribution of voids in amorphous hydrogenated carbon nitride films [9] and in a-SiC:H films [10,11] have been investigated. This lack of experimental PAS measurements is probably due to the difficulties in the interpretation of the data for the complexity of the amorphous systems. PAS, on the other hand, permits a non-destructive analysis of films as a function of depth from the first surface layer to the interface with the substrate. Therefore, PAS can give a direct evidence of the homogeneity of the films with regards to the distribution of open volume defects. As the type of open volume defects varies for the different carbon based materials, we have also measured by PAS samples of high oriented pyrolytic graphite, commercial carbon and glassy carbon. These measurements will be compared with the results obtained for the amorphous carbon films.

## 2. Experimental

### 2.1. Film preparation

a-C films were obtained using high energy (30 keV) ion beam deposition methods [12,13] on mirror polished (001) silicon wafers, which were chemically cleaned with trichlorethylene in an ultrasonic bath. The ion beam is obtained from the decomposition of 99.99% pure methane in the ion source by means of an electronic arc. The ions are accelerated through an extracting electrode and then go through a magnetic steerer in order to separate the  $H^+$  ions from the remaining hydrocarbon ions. Finally, they arrive at a stainless steel deposition chamber kept under a vacuum of  $10^{-5}$  mbar, where the sample to be coated is located; no external heating is provided.

When the ions (mainly  $CH_3^+$  and  $CH_4^+$ ) arrive at the substrate surface they disintegrate giving carbon and hydrogen ions with the same velocity (which is a function of the initial accelerating voltage); the C atoms carry a kinetic energy 12 times greater than the H atoms. At these energies, the carbon range in silicon (calculated with the TRIM code) is about 60 nm, and the H range is only 10 nm. The Si substrate is progressively C enriched, while the H atoms remain near the surface giving therefore a free hydrogen amorphous carbon film.

### 2.2. Film characterization

The films so obtained were analyzed using Raman spectroscopy, PAS and electrical resistivity measurements. These experiments were performed in as-grown and annealed films. Samples were annealed in a vacuum of  $10^{-5}$  mbar, in 50°C steps from 300 up to 600°C for 20 min, in order to analyze their thermal stability.

The Raman spectra were taken using an Ar laser operating at 514.5 nm; the dispersed beam was analyzed in a 90° geometry.

The electrical resistivity of the films was determined from  $I$ – $V$  measurements. The thickness of the layers (about 450 nm) was large compared with the roughness of the substrate. The effect of the C–Si junction and the Si substrate was taken into account.

PAS was performed by a slow electrostatic positron beam [14] coupled with a High Purity Ger-

manium Detector. The Doppler-broadening of the 511 keV annihilation line was measured as a function of the positron implantation energy in the 0.06–18 keV energy range. The shape of the 511 keV annihilation line was characterized by the so-called  $S$  parameter. The  $S$  parameter is calculated as the ratio of the counts in the central area of the peak ( $|511 - E_\gamma| \leq 0.85$  keV,  $E_\gamma$  is the energy of the annihilation gamma ray) and the total area of the peak ( $|511 - E_\gamma| \leq 4.25$  keV). The Doppler-broadening of the 511 keV annihilation line  $\Delta E_\gamma$  is related to the electron-positron annihilating pair momentum component  $p_z$ , in the detector direction, by the relationship  $\Delta E_\gamma = p_z c/2$  where  $c$  is the light velocity. The  $S$  parameter reflects the fraction of positron annihilating with electrons of low momentum. An increase of the  $S$  parameter values with respect to a non-defected sample is an indication of positron annihilation in open volume defects. In condition of trapping saturation, the higher the  $S$  value, the larger the open volume defects (i.e., vacancy, divacancy, voids) in which positron annihilate. More details about PAS with Doppler-broadening technique can be found in Refs. [15,16].

### 3. Results

In previous papers, it has been established that our as-grown a-C samples consist of an amorphous network of  $sp^2$  and  $sp^3$  C–C bonds; from K-edge EELS measurements it was shown that about 60% of the atoms are in  $sp^2$  sites. A density of  $2.1 \pm 0.1$  g/cm<sup>3</sup> ( $\sim 0.93$  the density of graphite) was estimated from the plasmon peak at 25.6 eV in the low-loss region of the EELS spectrum [4]. In these samples, the H content is less than 5%.

Raman spectra of these amorphous carbon films present a broad band centered at about 1500–1520  $cm^{-1}$  (G-peak) with a shoulder at 1350  $cm^{-1}$  (D-peak). The Raman spectrum of crystalline graphite consists of a narrow band at 1580  $cm^{-1}$ . The spectra of glassy carbon and microcrystalline graphite, on the other hand, consist of two bands at 1580 and 1360  $cm^{-1}$  (the latter is due to the lack of long range order) whose width and relative intensity depend on the grain size of the graphite microcrystals (Fig. 1). When amorphous carbon samples are graphitized by

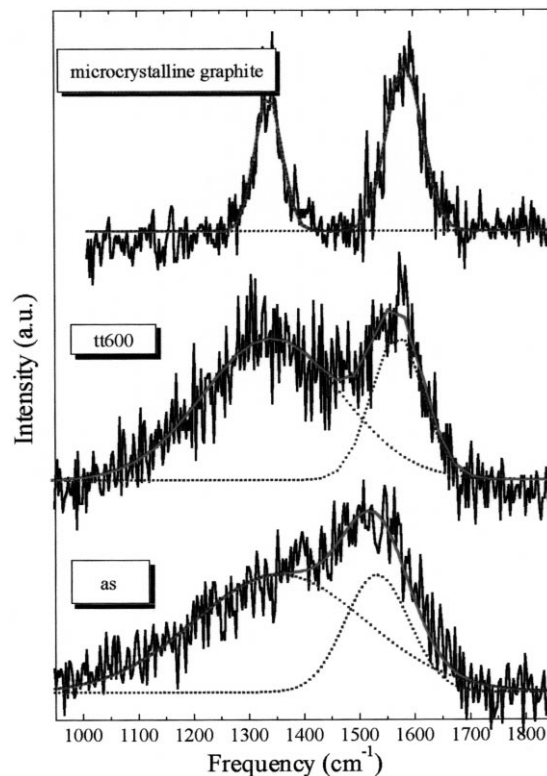


Fig. 1. Raman spectra of a-C film as-grown, annealed at 600°C and the commercial microcrystalline graphite.

thermal effects, their Raman spectra resemble those of glassy or microcrystalline carbon. For these graphitized samples, the plasmon peak in the low-loss region of the EELS spectrum shifts to 26.6 eV (the corresponding graphite peak is at 26.5 eV and therefore their densities are similar).

Fig. 2 shows the Raman spectra of the as-grown and annealed films. The results of the fittings with two Gaussian line shapes are shown in Table 1. As the annealing temperature increases, the two peaks become narrower and the G-peak shifts towards higher frequencies. At 450°C the G and D peaks reach the position characteristic of microcrystalline graphite denoting the presence of graphitic islands in the films. The  $I_D/I_G$  ratio of the graphitized samples provides information about the size and/or number of the graphitic islands [17–20]. Between 450 and 550°C the  $I_D/I_G$  ratio has a rather constant value of about 3.2 indicating that in this range of temperatures the average size of the graphitic islands re-

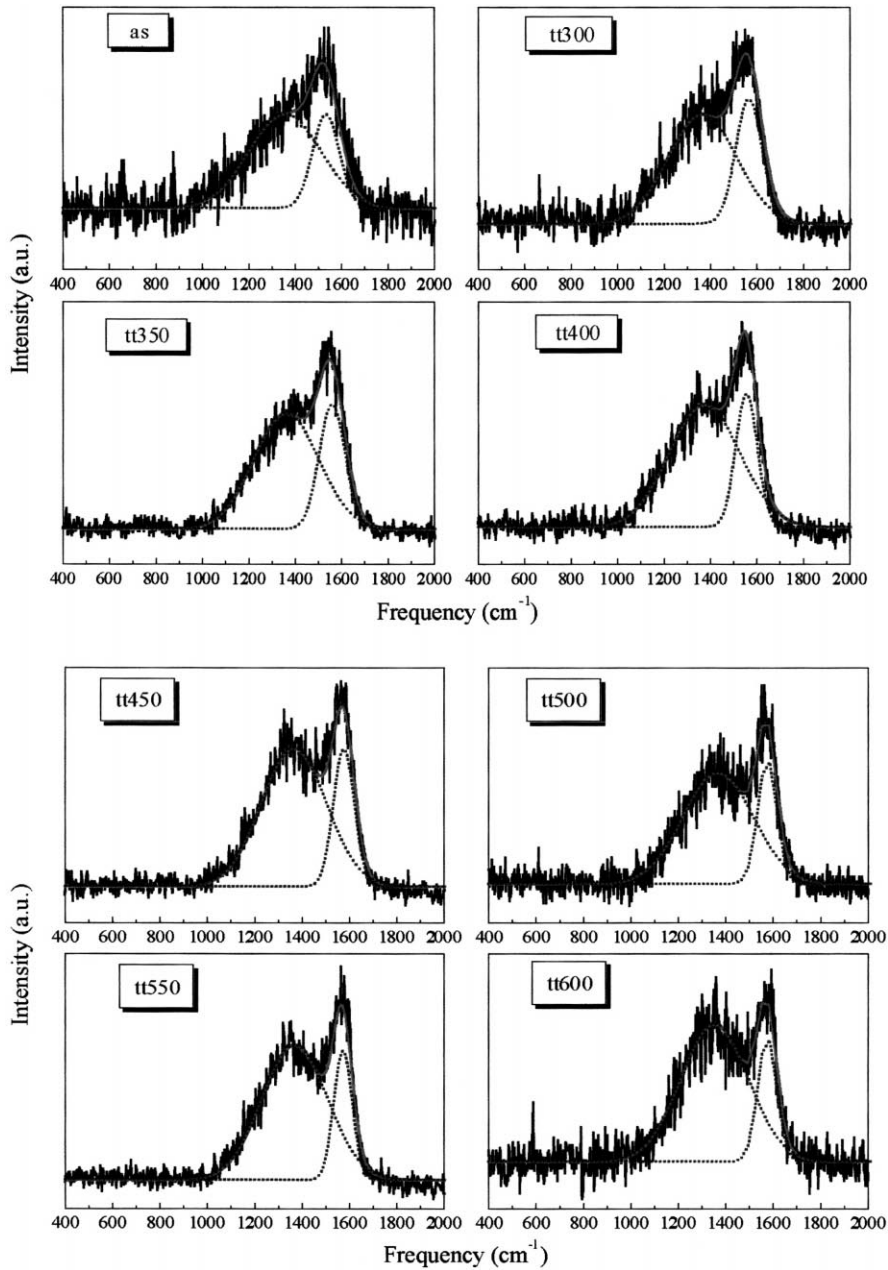


Fig. 2. Raman spectra of a-C films as-grown and annealed at different temperatures (300, 350, 400, 450, 500, 550 and 600°C) samples. Deconvolution with Gaussian line shape. (Experimental data: solid line; Gaussian fitting curves: broken line).

mains constant. This should suggest that up to 550°C there is a decrease in the bond angle disorder of the  $sp^2$  bonded atoms that organize in graphitic islands. At 600°C, however, this ratio grows reaching a value of 3.9.

The results of the electrical resistivity measurements as a function of the annealing temperature are shown in Table 2. As can be seen the as-grown films have a high resistivity ( $\sim 5 \times 10^9 \Omega \text{ cm}$ ), that falls to about  $20 \Omega \text{ cm}$  after annealing at 550°C, and

Table 1  
Experimental data taken from Raman measurements for the samples studied

Sample	$I_D/I_G$ ratio	Raman G-peak ( $\text{cm}^{-1}$ )	Raman D-peak ( $\text{cm}^{-1}$ )
as	2.45	1531	1355
tt300	2.27	1563	1364
tt350	2.31	1557	1360
tt400	2.52	1556	1363
tt450	3.09	1575	1364
tt500	3.29	1573	1366
tt550	3.13	1569	1358
tt600	3.91	1573	1351

reaches a value of  $\sim 1.5 \Omega \text{ cm}$  after annealing at  $600^\circ\text{C}$ .

The positron annihilation measurements for the as-grown sample and the samples annealed at 300, 400, 500, 550,  $600^\circ\text{C}$ , are shown in Fig. 3. The measurements at 350 and  $450^\circ\text{C}$  are not shown for the sake of clarity. The  $S$  parameter, normalized to the silicon  $S$  bulk value, is reported as a function of the mean positron stopping depth:

$$\bar{z} = AE^n/\rho, \quad (1)$$

where  $A = 3.5 (\mu\text{g}/\text{cm}^2 \text{ keV}^n)$ ,  $\rho$  is the density expressed in  $\text{g}/\text{cm}^3$  ( $\rho = 2.1 - 2.2 \text{ g}/\text{cm}^3$ , in our samples),  $n = 1.7$ . The positron implantation energy  $E$  is expressed in keV [16].

The variation of the mean positron depth, due to the increase of density (from 2.1 to  $2.2 \text{ g}/\text{cm}^3$ ) going from the as grown to the  $600^\circ\text{C}$  annealed sample, is of the order of the size of the points reported in Fig. 3.

First, we will describe the behavior of the  $S$  parameter with reference to the as-grown sample denoted by the star symbol in Fig. 3. The  $S$  parameter starts from a surface  $S$  value ( $S_s = 0.917$ ), then rapidly increases to reach the bulk  $S$  value typical of the as-grown film ( $S_b = 0.948$ ). The  $S_b$  value remains constant up to the interface with Si (shown with an arrow in Fig. 3) at about 450 nm. The reason for which the  $S$  curve rises monotonically between the  $S_s$  and the  $S_b$  value is that the fraction of positron diffusing back to the surface after thermalization decreases progressively with the increase of the implantation energy. On the other hand, the  $S$

parameter can be expressed as a linear combination  $S = p_s S_s + p_b S_b$  where  $p_s$  and  $p_b$  are the fractions of positron annihilating in a surface state or in a bulk state, respectively [16]. Thus, a rough estimation of the positron diffusion length  $L_+$  can be made looking at the depth corresponding to the  $S$  parameter at which the probability for a positron annihilation in a surface state or in a bulk state is the same:  $p_s = p_b = 0.5$ . From Fig. 3 we obtain  $L_+$  around 10 nm (a more accurate value will be given below). This is a very low value for the positron diffusion length if compared, for example, with the  $L_+$  value corresponding to the crystalline silicon ( $L_+ \cong 250 \text{ nm}$ ) [21]. A low diffusion length means that positrons are efficiently trapped by open volume defects. Finally, for higher positron implantation energy  $S$  increases again and reaches the reference  $S$  bulk value of silicon.

In the heat-treated samples and from Fig. 3, it can be observed that the film annealed at  $300^\circ\text{C}$  has the same behavior than the as-grown one. The  $S$  parameter of the annealed samples in the 350– $500^\circ\text{C}$  temperature range differs from the previous curves only in the first 20 nm and up to this depth the  $S$  parameter is lower than the  $S$  parameter corresponding to the as-grown and  $300^\circ\text{C}$  annealed samples. It could be also observed that in these first 20 nm the  $S$  parameter approaches the  $S_s$  value. At  $550^\circ\text{C}$  annealing temperature we observe a sharp decrease in the

Table 2

Second column: experimental data taken from electrical resistivity measurements for the samples studied. The associate error to these experimental determinations is about 30%. Third column:  $S$  bulk value for the measured sample, normalized to the  $S$  bulk value of silicon. The error associated with  $S_b$  is  $\pm 0.003$

Sample	$\rho (\Omega \text{ cm})$	$S_b/S_b$ silicon
As-grown	$\sim 5 \times 10^{10}$	0.948
tt300	$\sim 9 \times 10^9$	0.945
tt350	$\sim 9 \times 10^9$	0.946
tt400	$\sim 9 \times 10^9$	0.947
tt450	$\sim 2 \times 10^9$	0.945
tt500	$\sim 8 \times 10^8$	0.949
tt550	$\sim 20$	0.923
tt600	$\sim 1.5$	0.910
HPOG Graphite	–	0.883
Glassy carbon	–	0.952
Microcrystalline graphite	–	0.919

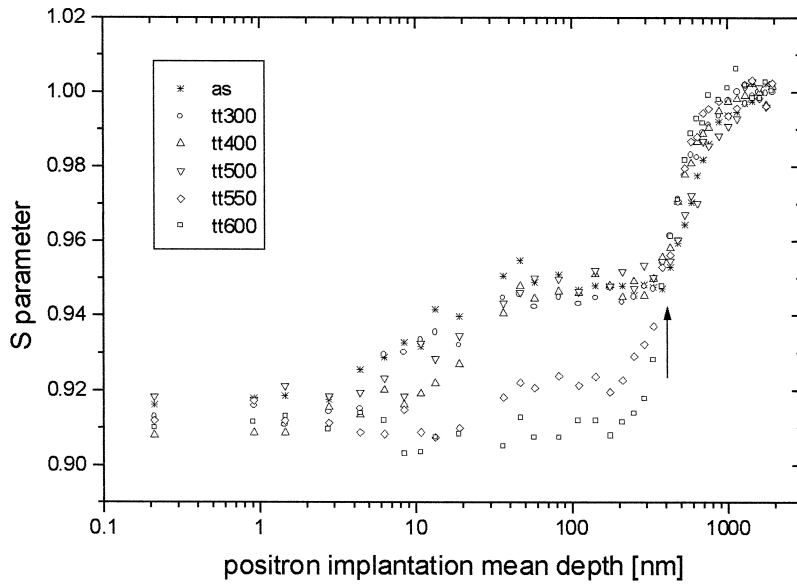


Fig. 3. Positron Annihilation Measurements.  $S$  parameter (normalized to the  $S$  bulk value of silicon) as a function of the mean positron implantation depth for the a-C films as-grown and annealed at different temperatures (300, 400, 500, 550, 600°C). The measurements at 350 and 450°C are not shown for the sake of clarity. The arrow indicates the interface between the carbon film and the silicon substrate.

$S_b$  value of the film: from 0.948 to 0.922. Finally, the  $S_b$  value, in the film thermally treated at 600°C, reaches the  $S_s$  value of the surface. At this temperature, the film is completely homogeneous in all its thickness but with a lower  $S_b$  value. This low value of  $S_b$  in comparison with the other  $S_b$  values is, as will be discussed, an indication of a distribution of smaller open volume defects.

For the discussion of the PAS data it is useful to know the behavior of positrons in carbon based materials. For this purpose we have measured the  $S$  parameter as a function of the positron implantation energy in the following materials: (a) in highly oriented pyrolytic graphite (HOPG) with the positron beam in the direction of the  $c$ -axis; (b) in commercial microcrystalline graphite; and (c) in glassy carbon. The PAS measurements are reported in Fig. 4 together with the  $S$  vs.  $E$  curve of the as-grown film already shown in Fig. 3. All the  $S$  data are normalized to the  $S_b$  value of silicon. To extract the positron diffusion length from the experimental data, the PAS data were analyzed by best fitting the  $S$  vs.  $E$  curves with the diffusion equation describing the positron motion in the steady state (details about the model and its application can be found in Refs.

[15,21]). The lines through the experimental points are the results of the best fitting procedures.

All the measured  $S$  curves of the samples shown in Fig. 4, start from an almost equal  $S_s$  value ( $\sim 0.92$ ). On the contrary, the evolution of the  $S$  parameter with respect to the mean implantation positron depth for each material is very different.

The  $S$  curve corresponding to the HOPG reaches smoothly a very low value in the bulk ( $S_b = 0.88$ ). As in this type of material, positrons are known to localize between the closely packed planes of graphite, this low  $S_b$  value can be related to the annihilation with the  $\pi$  electrons [22]. By using the diffusion model, a positron diffusion length  $L_+ = 102 \pm 6$  nm was estimated. Taking into account that the positron lifetime in graphite is  $\tau = 212$  ps [22], a positron diffusion constant  $D_+ = L_+^2 \tau^{-1} = 0.49$  cm<sup>2</sup> s<sup>-1</sup> can be obtained. The high  $S_s$  value in our HOPG sample could be attributed to imperfections existing in the first layer of the sample and consequently to the positron trapping in surface defects [23]. In fact, it was stated by two-dimensional angular correlation of annihilation radiation measurements on perfect surface, that the surface-bound positrons in HOPG annihilate with electrons which

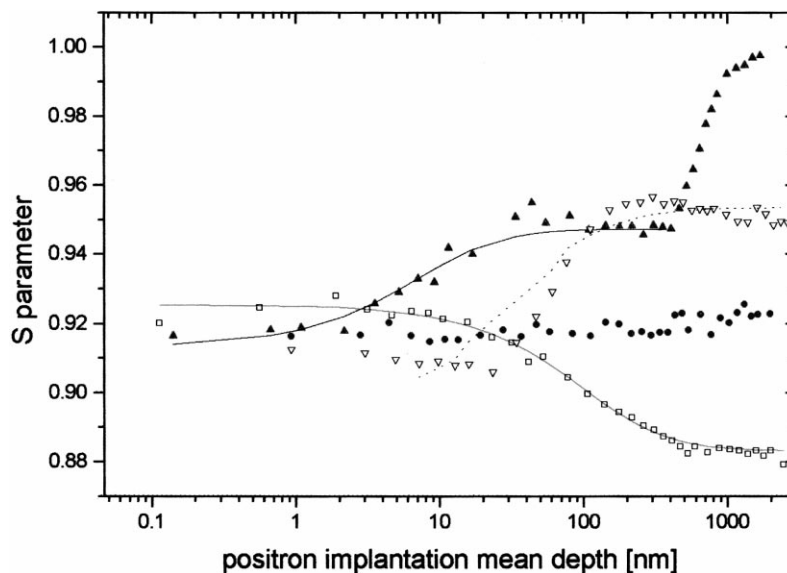


Fig. 4.  $S$  parameter as a function of the mean positron implantation depth for high oriented pyrolytic graphite (open squares), commercial microcrystalline graphite (full circles), glassy carbon (inverted open triangles) and the as-grown a-C film (full triangles). The lines through the experimental point are the best fit with the diffusion equation; see text for details.

are very similar to those found between the closely packed planes [24]. In this last case one would expect to measure the same  $S$  value for the surface and the bulk positron state.

As can be seen, the  $S$  curve for the commercial microcrystalline graphite is almost constant ( $S_b = 0.92$ ). In this material, positrons are efficiently trapped in the small open volume distributed through the amorphous carbon. Due to the fact that the  $S_s$  value is equal to the  $S_b$  value, we cannot evaluate the positron diffusion length in this case.

The evolution of  $S$  with the positron implantation mean depth corresponding to glassy carbon shows a very high  $S$  bulk value ( $S_b \cong 0.95$ ). It is worth noting that glassy carbon has a microstructure in which a big open volume, such as voids (from 1 to 4 nm in diameter [23]), is surrounded by carbon layers, and that its density ( $\rho \cong 1.5 \text{ g cm}^{-3}$ ) is very low compared with our carbon films or graphite. Therefore, the high  $S$  value in glassy carbon could be assigned to the positron annihilation in voids. The  $S$  curve, in the case of our glassy carbon sample, does not vary smoothly: after a slight decrease in the  $S$  value in the first 20 nm, it sharply increases to a high  $S$  value and finally a slight decrease is observed again. In this case, the diffusion model fails in fitting

such a sharp increase (see the dotted line in Fig. 4), nevertheless, a rough estimation of the diffusion length gives  $L_+ \cong 50\text{--}60 \text{ nm}$ .

Finally, the diffusion model applied to the  $S$  vs.  $E$  data of the as-grown film gives a positron diffusion length of  $L_+ = 7.5 \pm 1.5 \text{ nm}$ . As can be observed in Fig. 4, the  $S_b$  value for the as-grown film is a little lower than the  $S_b$  value found for the glassy carbon.

In Table 2 we have reported the  $S_b$  value normalized to the  $S_b$  silicon value for the amorphous carbon film and for the other carbon systems. The  $S_b$  is constant in the a-C films as-grown and annealed in the 350–500°C temperature range, its value is slightly lower than the  $S_b$  value obtained for the glassy carbon. For annealing heat treatments at 550 and 600°C, the  $S_b$  value of the a-C films shows an important decrease; these values are close to that of commercial microcrystalline graphite.

#### 4. Discussion

The as-grown a-C samples show a typical Raman spectrum characteristic of amorphous carbon films,

with a high electrical resistivity value ( $\sim 10^{10} \Omega \text{ cm}$ ). From PAS measurements, the constancy of  $S_b$  means that the film is homogeneous and that the open volume defects have a homogeneous distribution through the film.

To discuss the evolution of the films with the heat treatments, the experimental results have been divided, according to the annealing temperature range.

(a) Films annealed up to  $400^\circ\text{C}$  show no significant changes in the Raman spectra and in the electrical resistivity. On the other hand, a uniform distribution of open volume defects has been detected by PAS in the as-grown film and in the films annealed at  $300$  and  $350^\circ\text{C}$ . Probably these open volume defects can reach large sizes ( $\sim 1 \text{ nm}$ ). It can be guessed from the high  $S_b$  value, very near to the  $S_b$  value of glassy carbon [23]. From the positron point of view, the microstructural modification of the films starts from the surface at the annealing temperature of  $400^\circ\text{C}$ . This last finding is unique and it is possible thanks to the capability of the positron technique to probe different layers in a non-destructive way.

(b) In the annealing heat treatments from  $400^\circ\text{C}$  Raman spectra show that the graphitization process starts in the films at about  $400$ – $450^\circ\text{C}$ . This process is also reflected in a change of the electrical resistivity: it becomes about five times lower than the high value found in the as-grown film, but it is still far from the corresponding resistivity of a graphitic material. This could be an indication that  $\text{sp}^2$  clusters are organizing but the existing  $\text{sp}^3$  bonds remain stable.

(c) In the annealing heat treatments from  $500$  to  $550^\circ\text{C}$ , an abrupt change in the resistivity value is observed: it falls from  $8 \times 10^8$  to  $20 \Omega \text{ cm}$ . Finally, at  $600^\circ\text{C}$  it falls to  $1.5 \Omega \text{ cm}$ , somewhat higher than the resistivity of commercial microcrystalline graphite with a grain size of  $\sim 7 \text{ nm}$  ( $0.2 \Omega \text{ cm}$ ). For the same annealing temperature, the Raman  $I_D/I_G$  ratio increases; this fact, together with the abrupt change in the electrical resistivity would suggest that the  $\text{sp}^3$  bonded carbons begin to organize in  $\text{sp}^2$  clusters. An  $I_D/I_G$  ratio about 3.9 means that the size of the graphitic clusters is about  $1.2 \text{ nm}$  [25]. From PAS measurements, we can affirm that most probably the open volume defects decrease in size. The defects seen by PAS change abruptly at  $550^\circ\text{C}$ , in coincidence with the large decrease in the resistiv-

ity. At  $600^\circ\text{C}$  the defective structure is changed definitively, and resembles that monitored in the commercial microcrystalline graphite. The decrease in size of the open volume defects is also in agreement with the increase in the density of the annealed carbon films, similar to that of microcrystalline graphite.

## 5. Concluding remarks

On the basis of the information obtained by means of the experimental techniques used in the present work, it seems possible to find out a fine picture of the microstructural modification of the as-grown film as a function of the annealing temperature. The modification of the material seems to involve separately the two fractions of  $\text{sp}^2$  and  $\text{sp}^3$  carbon bonds.

As stated in Ref. [4], the microscopic structure of the as-grown film is an amorphous  $\text{sp}^3$  matrix in which graphitic clusters are embedded. Positrons have a very large mobility in carbon structures like graphite, as seen before, and diamond [26]. So, the large open volume defects in which they are efficiently trapped are probably localized in the  $\text{sp}^3$  matrix and at the interface of the  $\text{sp}^2$  clusters and the  $\text{sp}^3$  matrix.

At  $400^\circ\text{C}$  the a-C film starts to graphitize, according to Raman measurements, but PAS only sees a change in the first  $20 \text{ nm}$  of the film and the resistivity does not change considerably. This behavior can be related to a modification of the  $\text{sp}^2$  clusters that begin to organize, while the  $\text{sp}^3$  bonds and the amorphous  $\text{sp}^3$  matrix do not change. The fact that only the  $\text{sp}^2$  clusters seem to be involved in the graphitization process in the  $400$ – $500^\circ\text{C}$  temperature range, supports the idea that the large open volume defects are mainly confined in the  $\text{sp}^3$  matrix.

When increasing again the annealing temperature, the  $\text{sp}^2$  clusters continue to order and the  $\text{sp}^3$  fraction begins to graphitize. At  $550^\circ\text{C}$  the large open volume defects start to disappear and the resistivity decreases abruptly. The defects, as seen by PAS, are now a fine distribution of inter-cluster vacancy-like defects.

In this work, PAS has demonstrated to give valid complementary information to Raman spectroscopy

in the study and characterization of amorphous carbon films. The knowledge of the void distributions is of fundamental importance to understand the microstructural evolution during thermal treatments. In fact, a complete picture of the rearrangement process of this type of material cannot be abstracted from the void distribution. Moreover, open volume defects can influence the mechanical as well as the electrical properties of the films. In future, this non-destructive technique can be successfully applied in the study of thin films, and the results correlated to other complementary techniques.

## References

- [1] Y. Lifshitz, *Diamond Relat. Mater.* 5 (1996) 388.
- [2] Y. Lifshitz, in: A. Paoletti, A. Tucciarone (Eds.), *Tetrahedral Amorphous Carbon (ta-C)*, Proc. Int. School of Physics 'Enrico Fermi', Course CXXXV (IOS Press, Amsterdam, 1997) p. 209.
- [3] S. Prawer, K.W. Nugent, Y. Lifshitz, G.D. Lempert, E. Grossman, J. Kulik, I. Avigal, R. Kalish, *Diamond Relat. Mater.* 5 (1996) 433.
- [4] R.G. Pregliasco, G. Zampieri, H. Huck, E.B. Halac, M.A.R. de Benyacar, R. Righini, *Appl. Surf. Sci.* 103 (1996) 261.
- [5] E.B. Halac, H. Huck, G. Zampieri, R.G. Pregliasco, E. Alonso, M.A.R. de Benyacar, *Appl. Surf. Sci.* 120 (1997) 139.
- [6] T.M. Wang, W.J. Wang, B.L. Chen, S.H. Zhang, *Phys. Rev. B* 50 (1994) 5587.
- [7] P. Asoka-Kumar, K.G. Lynn, D.O. Welch, *J. Appl. Phys.* 76 (1994) 4935.
- [8] F.L. Freire Jr., D.F. Franceschini, R.S. Brusa, G.P. Karwasz, G. Mariotto, A. Zecca, *J. Appl. Phys.* 81 (1997) 2451.
- [9] F.L. Freire Jr., C.A. Achete, R.S. Brusa, X.T. Meng, A. Zecca, G. Mariotto, *Solid State Comm.* 91 (1994) 965.
- [10] T. Friessnegg, M. Boundreau, P. Mascher, A. Knights, P.J. Simpson, W. Puff, *J. Appl. Phys.* 84 (1998) 786.
- [11] G. Brauer, W. Anwand, P.G. Coleman, J. Störmer, F. Plazaola, J.M. Campillo, Y. Pacaud, W. Skrupa, *J. Phys.: Condens. Matter* 10 (1998) 1147.
- [12] H. Huck, A. Jech, E.B. Halac, J. Nicolai, M.A.R. de Benyacar, R. Righini, *Nucl. Instrum. Meth. B* 84 (1994) 62.
- [13] H. Huck, E.B. Halac, J. Orecchia, M. Igarzabal, H. González, M.A.R. de Benyacar, XIV Congresso Brasileiro de Engenharia Mecânica, San Pablo, Brasil, 1997.
- [14] A. Zecca, M. Bettonte, J. Paridaens, G.P. Karwasz, R.S. Brusa, *Meas. Sci. Technol.* 9 (1998) 1.
- [15] A. Dupasquier, G. Ottaviani, in: A. Dupasquier, A.P. Mills Jr. (Eds.), *Positron Spectroscopy of Solids*, North-Holland, Amsterdam, 1995, p. 581.
- [16] P. Hautojärvi and C. Corbel, in: A. Dupasquier, A.P. Mills Jr. (Eds.), *Positron Spectroscopy of Solids*, North-Holland, Amsterdam, 1995, p. 491.
- [17] F. Tuinstra, J.L. Koenig, *J. Chem. Phys.* 53 (1970) 1126.
- [18] D.G. McCulloch, S. Prawer, A. Hoffman, *Phys. Rev. B* 50 (1994) 5905.
- [19] D. S Knight, W.B. White, *J. Mater. Res.* 4 (1989) 385.
- [20] R.O. Dillon, J.A. Woollam, V. Katkanant, *Phys. Rev. B* 29 (1984) 3482.
- [21] R.S. Brusa, M. Duarte Naia, A. Zecca, C. Nobili, G. Ottaviani, R. Tonini, A. Dupasquier, *Phys. Rev. B* 49 (1994) 7271.
- [22] H.E. Schaefer, M. Forster, R. Würschum, W. Krätschmer, K. Fostiropoulos, D.R. Huffman, *Mater. Sci. Forum* 105–110 (1992) 815.
- [23] M. Hasegawa, M. Kajino, H. Kuwahara, E. Kuramoto, M. Takenaka, S. Yamaguchi, *Mater. Sci. Forum* 105–110 (1992) 1041.
- [24] P. Sferlazzo, S. Berko, K.G. Lynn, A.P. Mills Jr., L.O. Roelling, A.J. Viescas, R.N. West, *Phys. Rev. Lett.* 60 (1988) 538.
- [25] J. Robertson, in: J. McHargue (Ed.), *Diamond and Diamond-Like Films*, NATO Advanced Study Institute, Pisa, Plenum, New York, 1990, p. 1.
- [26] A.P. Mills Jr., G.R. Brades, D.M. Zuckerman, W. Liu, S. Berko, *Mater. Sci. Forum* 105–110 (1992) 763.